Determination of Flash Floods Hazards and Risks for Irbid Governorates Using Hydrological and Hydraulic Modelling

Naheel Al Azzam and Mustafa Al Kuisi

The University of Jordan, School of Science, Department of Geology, Amman, Jordan.

Abstract

Irbid city has suffered from several flash floods over the past few years, which caused several damages to the infrastructure and to people's lives. In this study, an approach based on the integration of Geographic Information System, Watershed Modeling System, Hydrological Modeling System, and River Analysis System has been used to construct hydrologic, hydraulic, and floodplain models to detect the areas with the high risk of flooding. The Digital Elevation Model from Shuttle Radar Topographic Mission was used in WMS to delineate drainage networks and sub-catchments' characteristics. The hydrological modeling was carried out using rainfall data from fifteen meteorological stations obtained over thirty-eight years. The SCS curve numbers for the subcatchments were obtained for normal conditions according to the land use data and the soil types of the study area, and were calculated to be 85.7, 88.1, 83.6, 79.9, and 82.4, respectively. The peak flood discharge was calculated over 2, 10, 25, 50, 100 and 1000-Year return periods. The hydraulic modeling carried out by the HEC-RAS model is based on the hydrographs resulting from the hydrological modeling, and steady-flow simulations were performed for the return periods of 2, 10, 25, 50, 100, and 1000-Years. Different scenarios for the maximum water surface profiles were constructed for each return period for the twenty main channels in the study area. The results showed that the volume of the flooded water will exceed the wadi banks for the 100- and 1000-Year rainfall return periods and flood inundation will occur.

1. Introduction

Natural hazards are events capable of causing significant damage to the natural and built environment. Flood is probably the most damaging, common, and frequent natural hazard in the world. In Dry lands such as Jordan, flash floods caused by storms of high intensity and short duration are common and are associated with heavy rainstorms which could be considered as the most frequent widespread and disastrous natural hazard in Jordan in the last decade (Youssef and Hegab, 2019). Recently, flash-flood problems in Jordan have largely increased due to different factors such as the continuous changing in land use/land cover due to inadequate enforcement laws, urbanization activities' expansion in flash-flood prone areas, low-quality constructions, and the increasing of the urbanization density. It is expected that; flood damages will increase over the years due to the previous different factors mentioned in addition to the effects of global climate change (Ibitoye, 2020). Therefore, it is necessary to define a methodology to predict flash floods in any region and predict the best method to protect the urban areas against inundations. The most common method to determine flash floods occurrence and the relationships between rainfall and runoff data is the River Analysis System (HEC-RAS) modeling (Derdour et al., 2017). Nowadays, flood hazard assessments have been improved due to the use of Geographic Information System (GIS) in integration with hydrological and hydraulic modeling. The GIS environment has the capability to extract the hydrological parameters, indispensable and morphometric characteristics from a high-resolution Digital Elevation Models (DEM), including catchments delineation, catchment shape, flow directions, slopes, longest path, and stream orders (Derdour and Bouanani, 2019). Moreover, it is necessary to make an assessment of flood-affected areas resulting from extreme precipitation and change in land use which can be helpful for a better understanding of the flood events (Derdour and Bouanani, 2019).

Non-accurate determination of rainfall and the hydrologic data and statistics are among the difficulties of estimating flood properties in basins, especially in arid regions such as Jordan. Recently, it is a routine approach to use models to simulate rainfall–runoff, to access flood properties, including time to-peak discharge. Therefore, the calibration and assessment of models are inevitable and necessary tasks. WMS is a conceptual model, which consists of different methods, including TR-55 (Technical Release 55), TR-20, SCS, and HEC-HMS (Hoseini et al., 2017).

Few studies in Jordan have dealt with flash floods using hydrologic and hydraulic modeling. Abu Islaih et al. (2020) conducted a comprehensive study and analysis of the main reasons which caused the flash flood in the Zarqa Ma'in area on October 25th, 2018. They calculated the runoff values for Zarqa Ma'in catchment area using the Soil Conservation Services (SCS) method, the hydrological modeling in Watershed Modeling System (WMS 11), and Geographic

Information System (ArcGIS 10.7). Farhan and Anbar (2016) conducted a study to assess the flash flood in Wadi Yutum watershed, southern Jordan. The assessment was conducted using remote sensing and the Geographical Information System (GIS) techniques combined with geomorphic and geological field data to test the probability of the risk of flooding spatially. Al-Weshah and El-Khoury (1999) described a flood analysis model developed and calibrated for the Petra catchment, using this model, flood volumes and flows have been estimated for storm events of different return periods.

Other studies integrated the hydrological and hydraulic models with GIS to predict the flood prone areas in arid regions. Abu El-Magd et al. (2020) used a multi-criteria process combined with the Geographical Information System (GIS) and remotely sensed data to produce a flash flood susceptibility map in Awlad Toq-Sherq, Southeast Sohag, Egypt. Niyazi et al. (2020) assessed runoff and reservoir capacity of the Jazan Basin in different return periods of rainfall events based on integrations between Watershed Modeling System (WMS) and the Hydrological Modeling System (HEC-HMS) in addition to the Geographic Information System (GIS). Abu-Abdullah et al. (2020) created a flood risk management program for Wadi Baysh Dam in Jizan Region, Saudi Arabia by integrating hydrologic and hydraulic models. Derdour and Bouanani (2019) used HEC-RAS and HEC-HMS in combination with the Watershed Modeling System (WMS) and the Geographic Information System (GIS) for rainfall runoff modeling and evaluating flood plain inundation maps in Ain Sefra city, SW of Algeria. Marko et al. (2019) used the GIS, WMS and HEC-RAS programs for hydraulic simulation, to present a two-dimensional flood inundation modelling in urbanized areas in Wadi Qows, Jeddah City, Saudi Arabia. Echogdali et al. (2018) compared the results of two methods used for delineating the extent of flooding in El Maleh Basin, Morocco. The first method was based on the integration of WMS and HEC-RAS. The second method is the Flood Hazard Index (FHI) method. El Alfy (2016) integrated the Geographic Information System (GIS), remote sensing, and rainfall–runoff modeling, to assess the impact of urbanization on flash floods in the arid southwest of Saudi Arabia. Sadrolashrafi et al. (2008) integrated GIS and WMS with commercial standard hydrological and hydraulic models, including HEC-1, HEC-RAS to modulate flooding in the Dez River Basin in Iran.

Irbid city, similar to other cities in Jordan, has suffered from several flash floods over the last few years. On 26-04-2018, the Civil Defense Forces rescued 1,000 factory workers who were surrounded by water. Moreover, in Ramtha city, several houses raided by floodwaters were evacuated, while several electricity poles fell to the ground (WFP, 2019). These flash floods, have caused several damages to the infrastructures and lives. Property damage may include houses, rooms, vehicles, and other property that came in contact with flood waters, in addition, homes that were flooded can be susceptible to harmful molds. Vehicles that were submerged usually have irreparable water damage to the engine and other critical components. Therefore, reliable

predictions are one of the key challenges for successful flash flood management in any catchment area (Pregnolato, 2017).

Two years ago, Jordan faced two waves of flash floods that took the lives of twenty-one people; most of which were children, near the Dead Sea. In addition, at least twelve people were killed after a heavy rainfall that triggered flash flooding in other several areas of the country, including Madaba region and Petra city, in addition, to the evacuation of nearly 4,000 tourists from the ancient city of Petra. These two accidents have raised flags for immediate actions and more focus on flash floods as a serious concern in Jordan (WFP, 2019).

2. Methods

2.1 Location and Climateq

Irbid city is located in the northern part of Jordan in Irbid governorate (Figure 1). Irbid city is one of the major cities in Jordan and the second most populated area in Jordan; 19% of Jordan's population live in Irbid governorate (DOS, 2018). Irbid governorate is approximately 1572 km^2 in size, and includes nine districts. According to the department of Statistics in Jordan, 83% of the Irbid population live in urban areas.
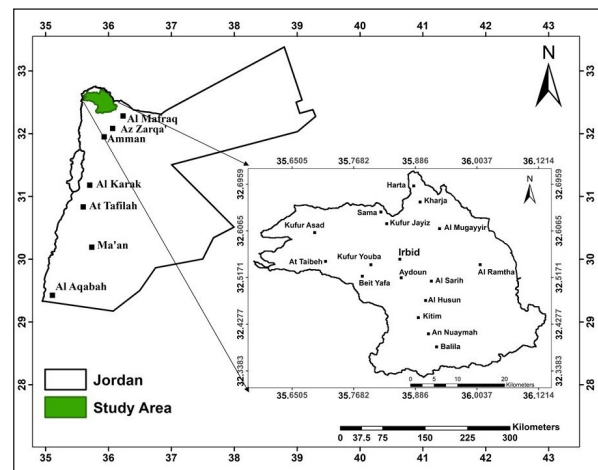

Figure 1. Location of the study area.

There are seventeen hospitals, sixteen universities and colleges, and 927 schools (DOS, 2020). Between 2015 and 2019, the total population of Irbid governorate had increased from 1.77 million inhabitants occupying around 356 thousand households to 1.92 million inhabitants occupying around 400 thousand households (DOS, 2020). The city of Irbid faced a large demographic growth and changes over the years, which involved the arrival of Palestinians, Iraqis, Syrians, economic migrants from Egypt, Asia, and elsewhere (UNHCR, 2018). In addition, many Jordanians moved there to receive education at the universities of Irbid gevernorate. The city has witnessed a significant increase in urban sprawl on agricultural areas in recent years due to the growth in population following the refugee movement from the neighboring countries of Syria and Iraq. The rates of urban expansion for Irbid governorate during the period (2003–2015) showed that the annual rates of municipal land transformation into urban area were around 1% of the municipalities' lands; 12% of Irbid lands were changed into urban area by 2015. The annual rate of land transformed into urban areas was around 1% during this period; this rate of

urban expansion takes place mainly on agricultural lands. The annual loss of Irbid's agricultural lands is about 2% (Al-Kofahi et al., 2018).

The climate of Irbid region is classified as semi-arid, with cold, rainy winters and dry, warm summers extending from May until October. The mean annual temperature is around 24 °C in the summer season, and about 8 °C during winter (Abdulla and Al-Qadami, 2019). The average annual precipitation ranges between 488 mm over the highlands to the west and southwest of Irbid, and 156 mm to the East (near Mafraq). The potential evaporation ranges from 2000 mm/year in the northwest, to 2400 mm/year in the southwest of the catchment (Hyarat, 2016).

The study area is about 1170 Km^2 which covers 74.5% of Irbid governorate. This area resulted from the watershed delineation of the Digital Elevation Model (DEM) using the WMS software package V.11. Figure (2) shows the DEM with 12.5m resolution from Shuttle Radar Topographic Mission (SRTM) dataset. The elevations in the watersheds of the study area range from around 267 m below sea level (bsl) in the western parts to 1194 m above sea level (asl) on the southwestern highlands near Ajlun area. As the slopes vary between 0-43°, the plain surfaces with slopes less than 4° occupy the eastern parts and cover more than 50% of the area. The land surfaces with slopes greater than 20° are found in the mountainous regions in the North (next to Hartha and Kharja) and to the West of the study area; they are mainly oriented North and Northwest as shown in Figure (3).
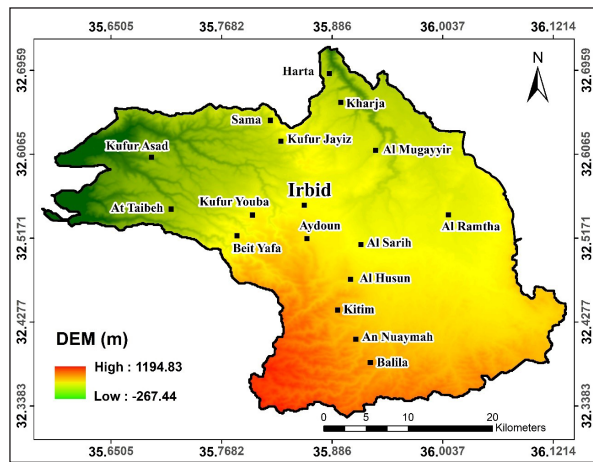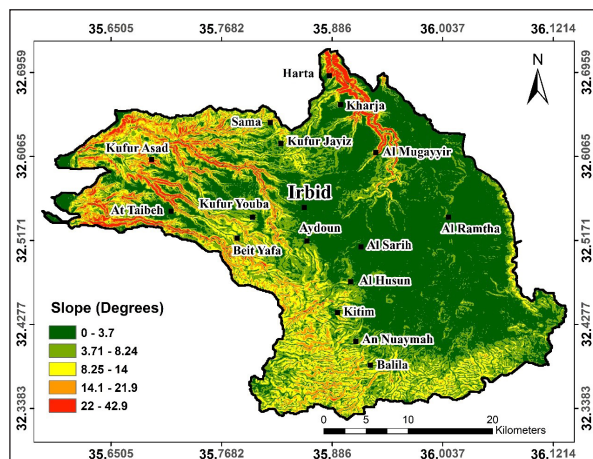
2.2 Land Use Land Cover Cover and Soil

A land use land cover map of the study area was prepared on the basis of a google earth map of 2019, and was reclassified as shown in Figure (4). Most of the land is field crops covering 26.1% of the study area, forests cover 9.4%, tree crops cover 16%, the urban fabrics cover 24.3%, the pastures cover 17%, bare rocks cover 3.6%, bare soil covers 3.5%, and the remaining 0.1% area is water bodies (Wadi Al-Arab dam). The urban areas with high population densities are mainly located in the middle and northeastern parts of the study area, while the remaining parts of the study area are characterized by a low population density.
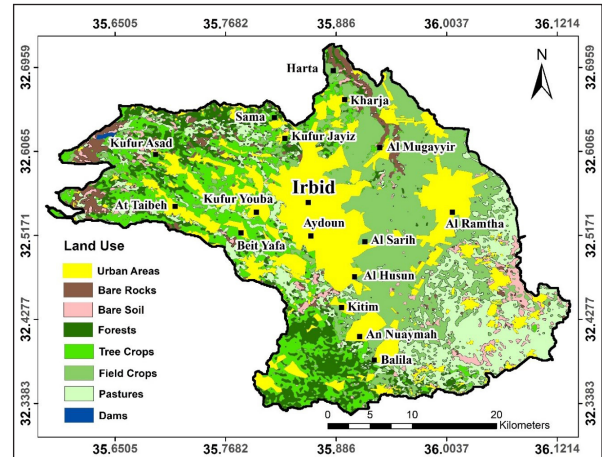

Figure 4. Land use map of the study area based on a google earth map of 2019.

The soil map of the investigated area was prepared after a detailed study of the soil profiles created by the Ministry of Agriculture for the study area. According to the classification of soils from the Ministry of Agriculture in Jordan there are seventeen nomenclature soil types (HTS and SSLRC, 1993). However, the Ministry of Agriculture in Jordan have created and produced three levels of soil maps. The soil map for the study area was taken from level 1. According to level 1 soil map, there are eight soil types present in the study rea. Moreover, these soil types were reclassified according to their texture in order to be used for the SCS curve number method (Figure 5). After that, each type of soil was assigned to its hydrological soil group created by US Soil Conservation Service (SCS) depending on permeability and infiltration and the resulting four groups are A, B, C, and D (SCS, 1986). The final soil map according to the Hydrological Soil Groups (HSG) is shown in Figure (6).
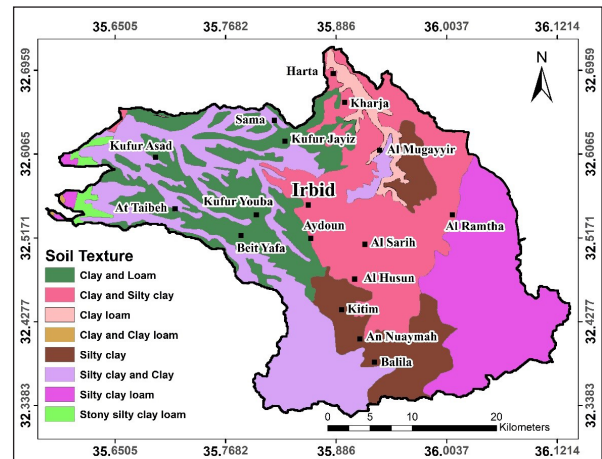

Figure 2. Digital Elevation Model of the study area.

Figure 3. Slope map of study area.

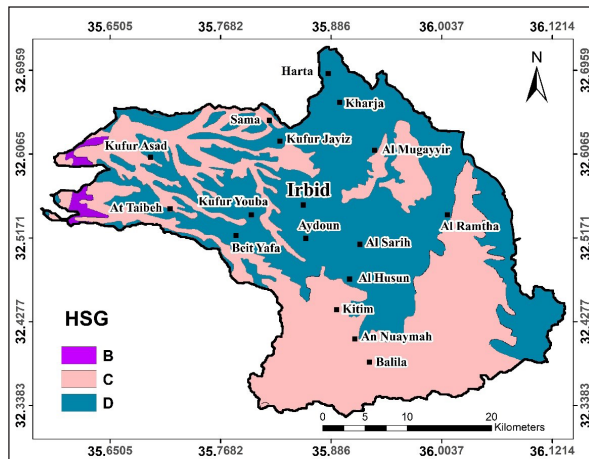**Figure 5.** Soil textures map of the study area.

Figure 6. Hydrological soil map of the study area.

2.3 Geological and Hydrogeological Setting

A sequence of more than 1000m of sedimentary rocks is well-exposed in the study area ranging in age from Upper Cretaceous to Recent. This sequence is subdivided into many geological formations, as described in the detailed geological maps (1: 50,000) produced by the Geological Mapping Division in NRA. According to geological maps (Irbid 3155(II) and as Shuna Ash Shamaliyya 3155(III)) in 1:50,000 scale acquired from Natural resources authority, the study area is mainly dominated by sedimentary rocks of Late Cretaceous (Turonian) to Quaternary (Pleistocene). The sedimentary rocks are comprised mainly of limestone, chalky marl, chert, bituminous marl, phosphate, and Quaternary terrace, and river bed deposits. The later sediments are mainly composed of sand, silt, clay, debris of chalky marl and basalt of Quaternary to Neogene in age (Moh'd, 2000) as shown in Figure (7).
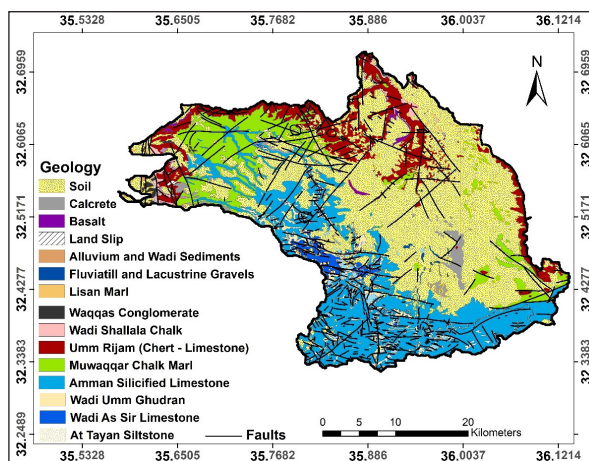

Figure 7. Geologic map of the study area (modified after Moh'd, 2000).

The study area is bounded to the west by the Jordan valley, a segment of the major rift structure recognizable from east Africa to South Turkey where a sinistral movement took place during the last 27 MA, with a proven horizontal movement slightly exceeding 100 km (Abed, 2000 and Moh'd, 2000). Regional dips are a few degrees towards the north, northeast, and northwest; high westerly dips accompanying the north-south step faulting associated with the rift formation are well-expressed in the western parts of the study area especially the Miocene Waqqas Conglomerate Group.

From a hydrogeological point of view, the main aquifer systems in the study area are: Wadi Shallala/Umm Rijam (B5/B4) and Amman/Wadi Es Sir Formations (B2/A7). These two aquifers are of excellent potential and are characterized by many wells for drinking and agricultural purposes.

3. Methodology

This study presents the application of Geographic Information Systems (GIS), Hydrologic and Hydraulic Models (WMS, HEC-HMS) to construct a hydrological model due to potential flash- flood hazards and to understand the relationship between rainfall depth and flood hazards at different return periods. The proposed methodology is listed through the next steps:

1- Catchment delineation, stream networks, and their characteristics by DEM processing, using ArcGIS and WMS modeling.

2- Finding out the CNs and the Intensity Duration Frequency (IDF) curves to be used in calculating the peak discharge.

3- Modeling rainfall/runoff relation, using HEC-HMS modeling in WMS, and extracting the unit hydrographs for different return periods (2, 10, 25, 50, 100, and 1000-Years).

4- Creating triangulated irregular network TIN for the study area using WMS.

5- Extracting cross-sections from the TIN in WMS.

6- Creating a conceptual model such as the river reaches, the stream centerline, the main channel banks, the cross-section lines, and the material zones which are called channel geometry using WMS.

7- Importing the results to be used as input data in hydraulic model HEC-RAS.

8- Defining the network schematic on HEC-RAS using Manning's roughness coefficients (n).

9- Applying a steady flow data which consists of peak discharge information, the reaches of boundary conditions, and flow regimes to compute the water surface elevation along the channel geometry.

10- Creating flood elevation maps with different return periods.

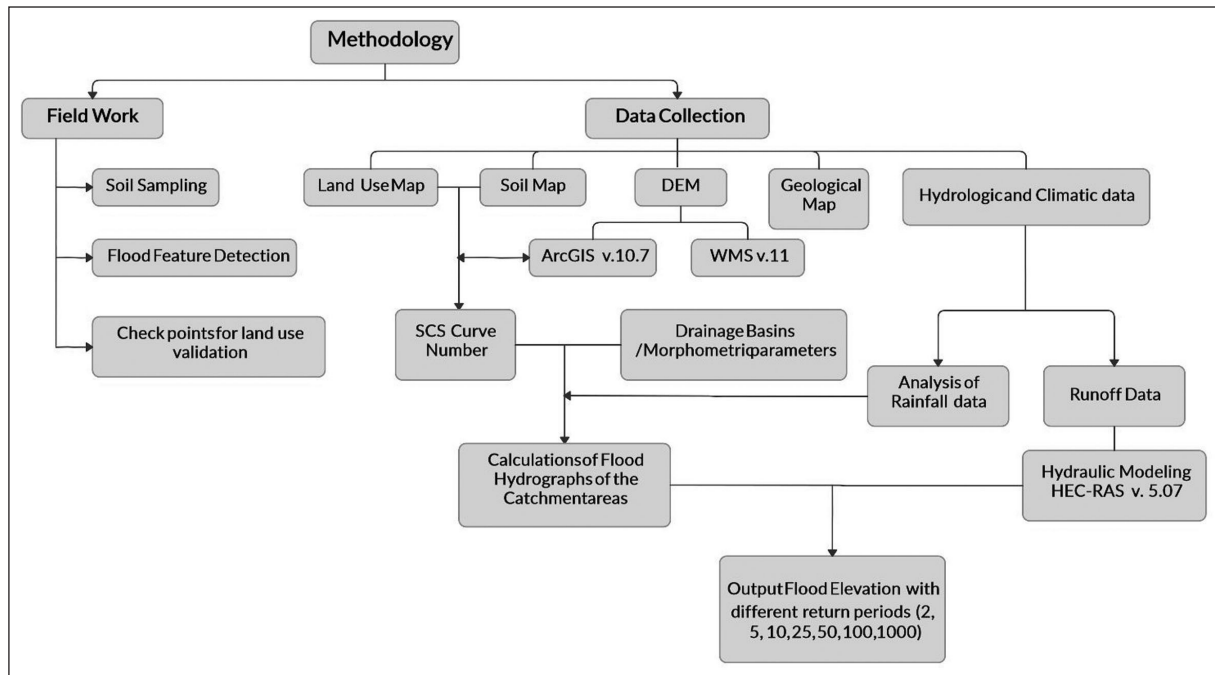The conceptual framework for the methods used is explicitly defined in Figure (8).

Figure 8. Schematic working flow of the used methodology.

4. Results

4.1 Catchment Delineation and Their Characteristics

To generate rainfall-runoff models, comprehensive information of the study area is required, including the topographic map to delineate drainage networks, catchment boundaries, flow paths, slopes and reach lengths, the WMS software was used to extract these parameters. The study area has been divided into five sub-catchments (B1, B2, B3, B4, and B5) as shown in Figure (9). The morphometric parameters of the sub catchments are shown in Table (1).

Table 1. Morphometric characteristics of the sub-catchments.

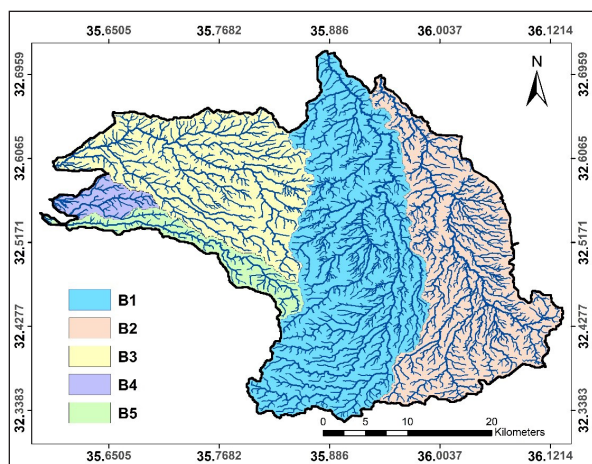| Sub-Catchment	Sub-Catchment Area Km²	Maximum Flow Distance (m)	Sub-Catchment Slope (m/m)	Maximum Flow Slope (m/m)
B1	448.62	66644.32	0.0923	0.0164
B2	351.49	52641.71	0.0500	0.0172
B3	276.26	41969.26	0.1415	0.0261
B4	29.52	14130.75	0.1503	0.0450
B5	64.03	37052.09	0.1788	0.0346

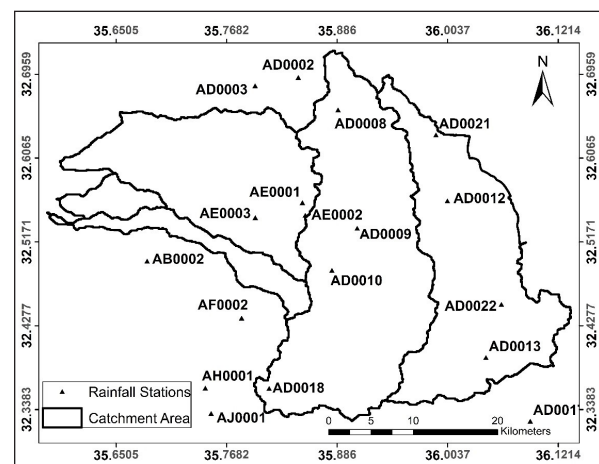**Figure 9.** Sub Catchments of the study area.

Figure 10. Rainfall Stations within and surrounding the study area.

4.2 Rainfall Frequency Analysis

The daily rainfall data for seventeen rainfall stations located inside and outside the study area were obtained from the database of the Ministry of Water and Irrigation (MWI). The location of rainfall stations is shown in Figure (10).

The daily rainfall data extends from 1980 to 2017, where the long-term average was calculated for each rainfall station. However, only fifteen rainfall gauge stations were selected to study and to be compared the climatic indication from meteorological parameters. During the past

two decades, there was an increasing trend in the rainfall amounts from east (ie: Hosha 156 mm/yr) to north west (Kufur Youba 457mm/yr) and south west (Rihaba 489mm/yr) for the study area. The highest average annual rainfall was registered at Rihaba Station (488.91 mm), whereas the lowest was recorded at Hosha Station (156 mm). In Hosha Station, there was a gradual decrease in the amount of precipitation over the last three decades, however there was an increasing trend in precipitation during the last ten years. Its maximum rainfall recorded was in 2013 with the amount of (327) mm. Moreover, in Kufur Youba Station, the trend of the rainfall data indicates a decrease in annual precipitation during the last three decades and its maximum rainfall recorded was 773 mm in 1992. In Rihaba Station, there is a gradual increase in the rainfall during the period (1982-1992) with a maximum rainfall of 1092.5 mm recorded in 1992. After that, during the last twenty-five years, there was a decrease in precipitation amounts. It is not surprising to see that precipitation was declining during that period as a result of climate change impacts which were very pronounced by the increasing desertification and the potential of sand and dust storms (SDS) in the region (Atashi et al., 2020).

The 3, 5, 7, 9, 11-year moving averages were calculated for each station. The eleven-year moving average mostly behaved as the long-term average line as shown in Figure (11).
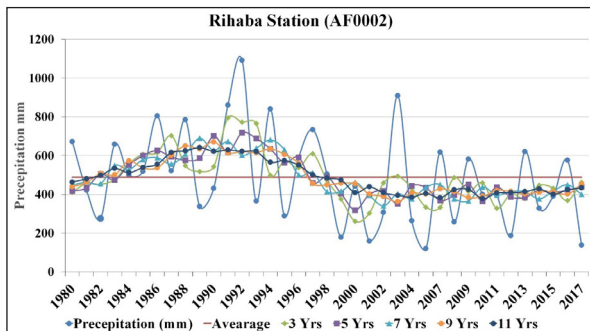

Figure 11. Moving averages calculated for Rihaba Station rainfall data.

The areal distribution of rainfall over the catchment areas was calculated by using the annual average rainfall for all rainfall stations and was illustrated by Isohyetal and Theissen polygon methods as shown in Figure (12 a and b). The WMS v.11 software has used the theissen polygon to calculate the maximum flood discharge in this study by taking the gauge weights.

It is clear that the rainfall records in the middle and west regions of the study area show high amounts of precipitation, while in the eastern parts there is a decreasing trend in the amount of precipitation (Figure 12 a). However, in the last ten years in the dry regions east of the study area, precipitation

amounts show an increasing trend. This high precipitation rates can be attributed to the consequences of climate change and the thunder storms characterized by high precipitation intensities with short periods.
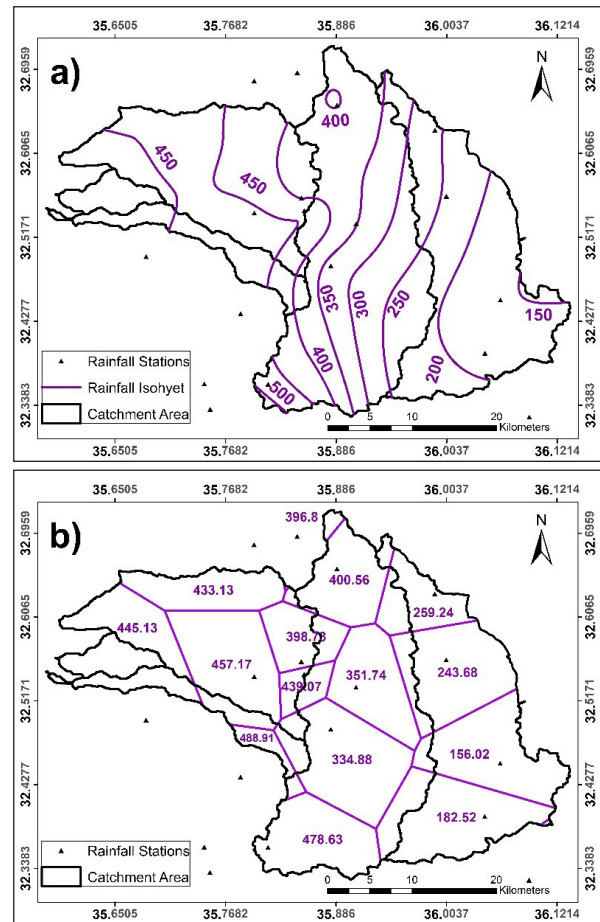

Figure 12. (a) Isohyetal and (b) Theissen polygon maps.

The rainfall Intensity-Duration-Frequency (IDF) curves show a graphical presentation of the possibility that certain rainfall intensity, duration, and return period will occur with similar characteristics. The IDF Curve is a graphical representation of the probability that a rainfall with a specific intensity and duration will occur within a given period of time. It is used to determine the frequency of a given precipitation in terms of its intensity and duration (Dupont and Allen, 1999). The daily rainfall depth and maximum records of rainfall stations are available over thirty-eight years for the seventeen gauge stations inside and outside the five sub-catchment area. Therefore, IDF curves were constructed using data from all stations and covering the period of 1980-2017. The IDF computations and IDF-curves were prepared for all rainfall stations; however, Irbid School Station was taken as an example and is illustrated in Table (2) and Figure (13).

Table 2. Rainfall Intensity (mm/min), Duration and Frequency at Irbid School Station.

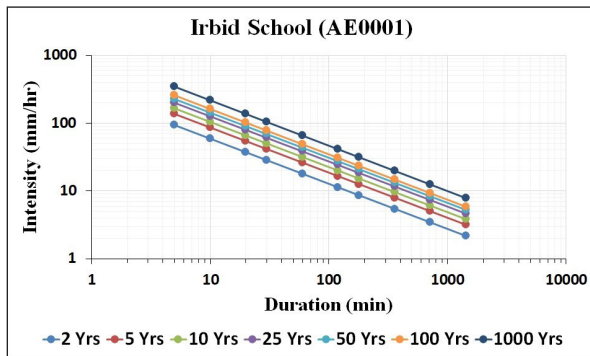| Return Period	Duration (min)									
	5	10	20	30	60	120	180	360	720	1440
2	93.52	58.92	37.12	28.33	17.84	11.24	8.58	5.40	3.40	2.14
5	136.72	86.15	54.26	41.41	26.09	16.43	12.54	7.90	4.98	3.14
10	165.33	104.17	65.62	50.08	31.55	19.87	15.17	9.55	6.02	3.79
25	201.47	126.94	79.96	61.02	38.44	24.22	18.48	11.64	7.33	4.62
50	228.28	143.84	90.60	69.14	43.56	27.44	20.94	13.19	8.31	5.24
100	254.90	160.61	101.17	77.21	48.64	30.64	23.38	14.73	9.28	5.85
1000	342.84	216.02	136.07	103.84	65.42	41.21	31.45	19.81	12.48	7.86

Figure 13. IDF Curve for Irbid School Station (Authours calculations).

Figure 14. Annual precipitation and runoff, runoff percentage from Irbid School Station.

4.3 Rainfall-Runoff Model Approach

The SCS curve number method is the most commonly used and efficient rainfall-runoff method for estimating the amount of runoff generated from rainfall data in any area. The method can be used to find average annual runoff values. The curve number is based on the area's hydrologic soil group, land use, and other factors affecting runoff and retention in a watershed and its values. The Curve Number (CN) is a dimensionless number defined as $0 \leq CN \leq 100$. For impervious and water surface CN=100, for natural surface $CN \leq 100$. The curve numbers for the five sub-catchments B1, B2, B3, B4, and B5 were calculated to be 85.7, 88.1, 83.6, 79.9, and 82.4, respectively. It is worth mentioning that when the precipitation storm/event is less than the computed initial abstraction (Ia), no runoff exists.

The standard SCS curve number method (SCS, 1986) is based on the following relationship between rainfall depth (p) and runoff depth (Q):

$$Q = (p - 0.2S)^2 (p + 0.8S) \quad \text{............................ (1)}$$

Where:

Q = the runoff depth (mm)

P = the precipitation depth in the same unit of the runoff (mm)

Ia = the initial abstraction (mm) =0.2S

S = the total losses of the rainfall depending on soil type (mm) and it can be found by the following equation:

$$S = \left(\frac{25400}{CN}\right) - 254 \quad \text{.. (2)}$$

The results of the computations of rainfall runoff relations discussed in the methodology are presented in Figure (14), which shows the annual runoff data for thirty-eight years (1980-2017) representing one of the main stations in the area, Irbid School Rainfall Station where the average runoff is equal to 65.62 mm/year.
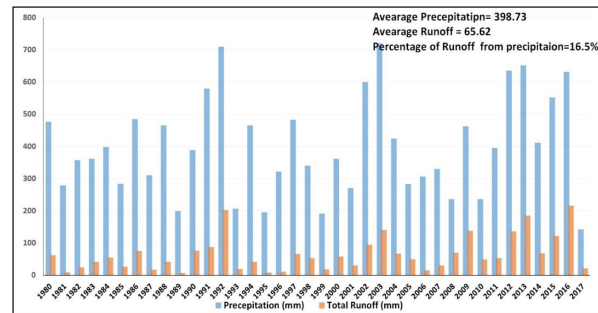
4.4 Unit Hydrograph

The unit hydrograph approach is used in this study to determine the peak discharge and its magnitude values. Results obtained by applying these applications are acceptable for hydrological simulation purposes. The unit hydrograph represents the catchment response to collect a unit rainfall excess of D-hour duration to produce the direct runoff hydrograph. By using the necessary basin parameters for running the hydraulic model, the peak flood discharge was estimated using HEC-HMS, SCS methods. The UH is multiplied by the effective rainfall out of the design storms at different return periods in order to produce the runoff hydrographs. The peak flood discharge was calculated by considering 2, 5, 10, 25, 50, 100, and 1000-Years return periods. Figure (15 a, b, c, d) shows results for sub-catchment B1 obtained using a fore method for different return periods. Figure (16) shows the peak flood discharge calculated considering the 2, 5, 10, 25, 50, 100 and 1000-Year return periods in different durations over twenty-four hours in sub-catchment B1.
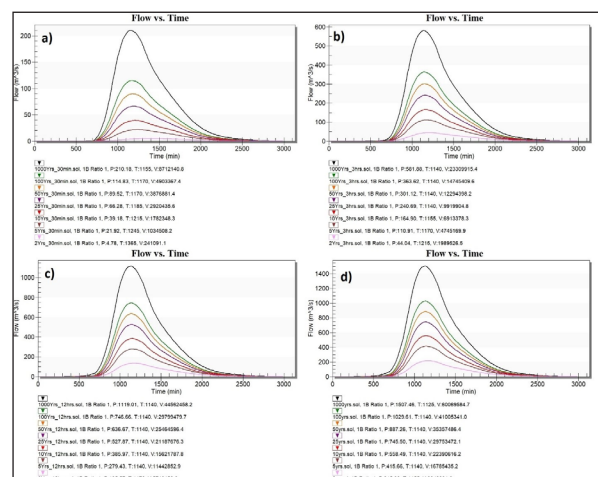

Figure 15. Unit hydrographs show the peak flood discharge estimated using HEC-HMS, SCS methods in sub-catchment B1 for different return periods in: a) 30 min. b) 3 hrs. c) 12 hrs and d) 24 hrs.
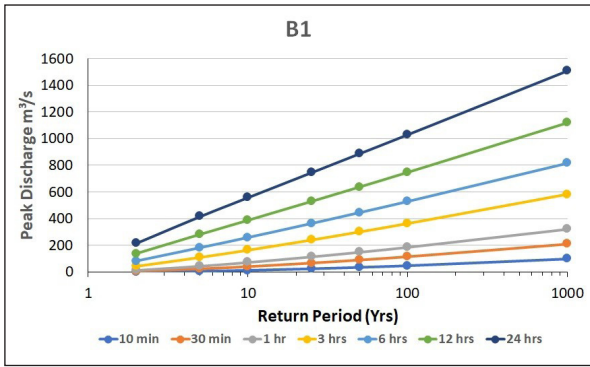
Figure 16. The peak discharge (m³/s) in different durations and return periods in B1.

4.5 Hydraulic Modeling Results

The hydraulic model (HEC-RAS) requires information about channel and floodplain geometry and Manning's roughness values. In this study, the input data for HEC-RAS were prepared using WMS and HEC-HMS. HEC-RAS represented the structure of the channel networks by a series of interconnected reaches. Three main geometry data required for HEC-RAS, consists of stream center line, main channel banks, and cross section cut lines. Twenty main channels divided into sixty reaches with well-defined junctions were extracted from the DEM in urban areas in the study area. Cross sections were constructed manually perpendicular to the flow lines of channels as shown in Figure (17). The twenty channels' networks and cross-sectional profiles were exported from WMS into HEC-RAS. The HEC-RAS model was run with detailed channel networks. It computes the depths based on the peak discharge computed by HEC-HMS at the determined cross sections and conducts interpolations along the reaches (Derdour and Bouanani, 2019).

The peak discharge data for each catchment was calculated with HEC-HMS, and were used as an input to the HEC-RAS for modelling water depths along the flood path. Data from all return periods, were imported and calculated by WMS. In HEC-RAS, the flood path is defined through about 1000 cross-sections extracted from the TIN of the study area. The initial model has on average 1 profile every 500 m. To have an even finer space step, cross profiles were created by interpolation of the extracted profiles, and a profile was added as soon as the distance between two profiles exceeded 200 m, so the flood path is defined through 40-45 cross-sections in each channel.

To make this study valuable for researchers, one example was taken for flood inundation plains, named Irbid A Channel, which represents an urban area upstream downtown zone located to the east of Irbid city (between Bushra and Hawwara). The cross-sections width ranges between 500 and 600 m for the main channel. Roughness coefficients (Manning n-values) were assigned to each cross-section in WMS, HEC-RAS. Coefficients were assigned using aerial photographs of the wadis, verified or adjusted by field observations and were almost determined based on the field visits. The USGS Guide for selecting Manning Roughness coefficients (Manning's n) for natural and flood plain was used in the study area. Roughness coefficients (Manning's n) used in the study area were 0.03 for river area, 0.10 for agriculture area, 0.08 for the urbanized area, and 0.04 for bare soil. In addition, the normal depth was the channel segment slope, and the flow regime in HEC-RAS is set to be mixed (Arcement and Schneider, 1989; Echogdali et al., 2018). The upstream and the downstream boundaries condition is set as a normal depth. After fulfilling all the input data and boundary conditions in HEC-RAS, the simulation was done as a steady-state analysis.
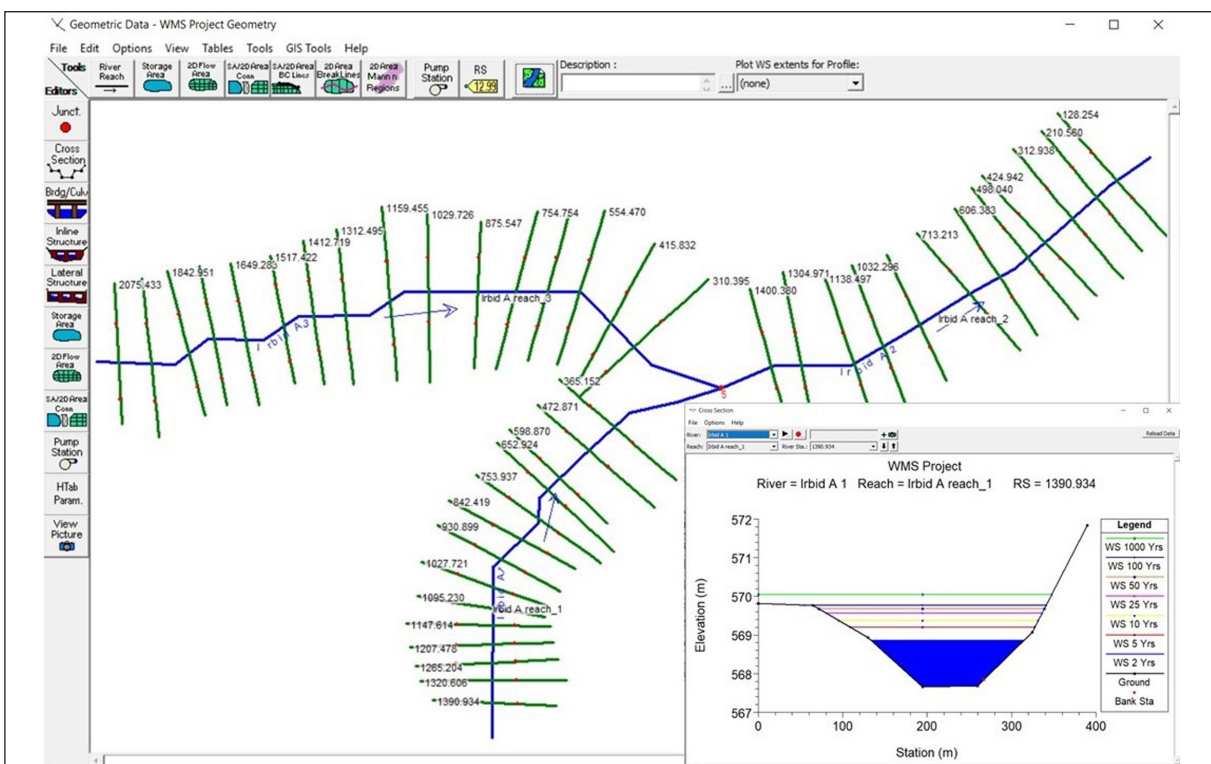

Figure 17. One of the channels and perpendicular cross sections in Irbid city (Irbid A channel).

Based on the hydrographs resulting from the rainfall runoff model, steady-flow simulations were performed for the return periods of 2, 10, 25, 50, 100, and 1000-Years. The peak discharge calculated by HEC-HMS was entered into HEC-RAS; the results were imported and prepared by WMS for all return periods. HEC-RAS interpolate the results of water-surface elevation data and delineate the flood inundation, as shown in Figures (18 and 19). This calculation revealed that the region most affected by the

flood is both upstream and downtown areas that is marked by low altitudes. The water depth in this area exceeds 2.43 m downstream for a two-Year flood and maximum depth of 3.3 m for 1000-Year flood. Moreover, the width of the flooded areas reached during the 100-Year flood and 1000-Year flood was 400 m and the 430 m, respectively. It is clear that the volume of the flooded water will exceed the wadi bank for the 100- and 1000-Year rainfall return period and flood inundation will occur.
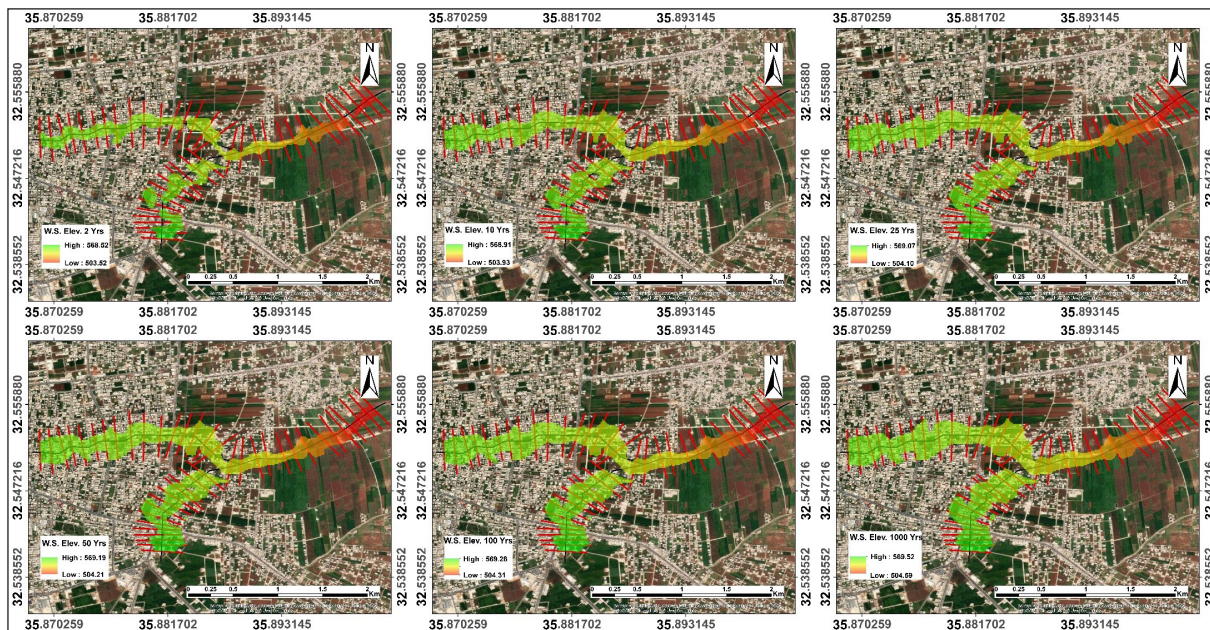
Figure 18. Flood inundation map, surface water elevation for Irbid (A) channel (return period 2, 10, 25, 50, 100, and 1000-Years).
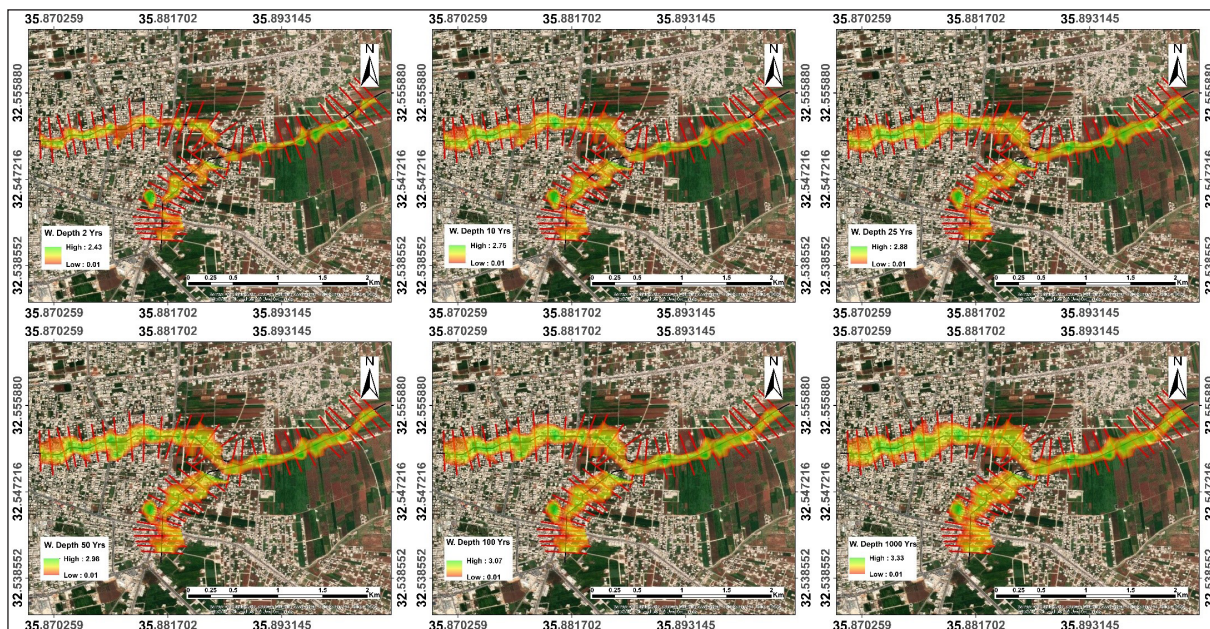
Figure 19. Flood inundation map, water depth for Irbid (A) channel (return period 2, 10, 25, 50, 100, and 1000-Years).

5. Discussions

The findings of flood depth assessment as indicated in Figure 19 revealed a significant increase in inundated areas in the study area. An increase of 2.4m (2-Yr) and 3.3m (1000-Yr) was detected in the area with flood depths greater than 0.9 m. As a result of the climate change impacts characterized by the intensification of rainfall, the inundated areas will increase.

Heavy and extreme rainfall represented by an exceedance of the average rainfall level can result in flooding. Irbid area is characterizing by flat area morphology with low slopes, a high population density, and intensive urban growth. In fact, heavy or persistent rains in the catchment area or the upper regions of the drainage system can lead to an excess of water

in the wadis and can create floods downstream. In addition, the growth of inundated areas will lead to an increase in the risk of the exposed built-up areas to flood. The increase in built-up areas will lead to an enhanced exposure of assets to flood water. The hydrologic modeling shows that flooding caused by more frequent rainfall events (with a smaller return periods and durations) is exacerbated more by urbanization than by large storm events. This can be seen more clearly in the southern and middle of the watershed, which might experience an increase in the discharge caused by the 2, 5, 10-year storms if fully urbanized. Urbanization, in general, will increase the peak discharge, the runoff volume, and the extent of the flooded area within a catchment. For urban areas, this means that more streets and built areas will be flooded and inundated as shown in Figure 20.

Figure 20. Inundated street in Irbid (A) channel area.

The impact will also depend on the terrain. For steep areas, the flooding will last for a shorter duration, but water velocities will be high. This can cause the vehicles on the streets to be swept away and may cause destruction due to the force of the water. Stagnant water on gentle slopes (Figure 21) also poses other threats, including water contamination. These findings are supported by several studies demonstrating that the increasing urban activities in flood plain areas will increase peak discharge, decrease the time to peak, and increase runoff volume (Almousaw et al., 2020; Mancini et al., 2020).

Figure 21. Stagnant water in Irbid (A) channel area.

6. Conclusions

The study area is subdivided into five sub-catchments B1, B2, B3, B4, and B5 with the areas of 448.6, 351.5, 276.3, 29.5, and 64 Km^2, respectively. The study presents a systematic approach to identify flash floods and their future risks based on the spatial extent of inundations in Irbid city.

The SCS curve numbers were obtained for normal conditions according to the LULC and the soil types of the study area; they were calculated to 85.7, 88.1, 83.6, 79.9, and 82.4. The peak flood discharge was calculated considering 2, 5, 10, 25, 50, 100 and 1000-Year return periods. The peak discharges at the sub catchments were calculated showing that the minimum discharge is 66.27 m^3/s at the sub catchment B4, 164.68 m^3/s at B5, 319.23 m^3/s at B2, 746.66 m^3/s at B1, and the maximum is 765.29 m^3/s at B3 for a (100-Year) return period.

The hydraulic modeling carried out by the HEC-RAS model based on the hydrographs resulting from the hydrological modeling steady-flow simulations was performed for the return periods of 2, 10, 25, 50, 100, and 1000-Years. Different scenarios for the maximum water surface profiles were predicted for each return period for twenty main channels in the study area. It is proven that the area will suffer from flood hazards and infrastructure damages.

References

Abed, A. (2000) Geology of Jordan (In Arabic). Dar Wae'l publication 550p. Amman, Jordan.

Abdulla, F. A., and Al-Qadami, A. (2019). "Structural Characteristics of in Jordan." In Patterns and Mechanisms of Climate, Paleoclimate and Paleoenvironmental Changes from Low-latitude Regions. In: Zhang, Z., Khelifi, N., Mezghani, A., Heggy, E. (Eds.), GAJG 2018.   Advances in Science, Technology and Innovation. 103–105. Cham: Springer. https://doi:10.1007/978-3-030-01599-2_24.

Abu-Abdullah, M. M., Youssef, A. M., Maerz, N. H., Abu-AlFadail, E., Al-Harbi, H. M., Al-Saadi, N. S. (2020). A Flood Risk Management Program of Wadi Baysh Dam on the Downstream Area: An Integration of Hydrologic and Hydraulic Models, Jizan Region, KSA. Sustainability 12(3): 1-24. https://doi:10.3390/su12031069.

Abu El-Magd, S. A., Amer, R. A., Embaby, A. (2020). Multi-criteria decision-making for the analysis of flash floods: A case study of Awlad Toq-Sherq, Southeast Sohag, Egypt. Journal of African Earth Sciences 162: 103709. https://doi: 10.1016/j.jafrearsci.2019.103709.

Abu Islaih, A., Yaghan R., Al Kuisi M., Al-Bilbisi, H. (2020). Impact of Climate Change on Flash Floods Using Hydrological Modelling And Gis: Case Study Zarqa Ma'in Area. International Journal of Applied and Natural Sciences 9(5): 29–52.

Al-Kofahi, S., Hammouri, N., Sawalhah, M., Al-Hammouri, A. Aukour F. (2018). Assessment of the urban sprawl on agriculture lands of two major municipalities in Jordan using supervised classification techniques. Arabian Journal of Geosciences 11: 45. https://doi.org/10.1007/s12517-018-3398-5.

Almousawi, D., Almedeij, J., Alsumaiei, A.A. (2020). Impact of urbanization on desert flash flood generation. Arabian Journal Geosciences 13, 441. https://doi.org/10.1007/s12517-020-05446-z.

Al-Weshah, R. A. and El-Khoury, F. (1999). Flood Analysis and Mitigation for Petra Area in Jordan. Journal of Water Resources Planning and Management 125(3): 170–177. https://doi:10.1061/(asce)0733- 496(1999)125:3(170).

Atashi, N., Rahimi, D., Al Kuisi, M., Jiries, A., Vuollekoski, H., Kulmala, M., Vesala, T., Hussein, T. (2020). Modeling Long-Term Temporal Variation of Dew Formation in Jordan and Its Link to Climate Change. Water 12(8): 2186.
 https://doi:10.3390/w12082186.

Arcement, G. J. and Schneider, V. R. 1989. Guide for Selecting Manning's Roughness Coefficients for Natural Channels and Flood Plains (U.S. Geological Survey Water Supply Paper 2339). U.S. Geological Survey.

Brunner, G. and CEIWR-HEC (Hydrologic Engineering Center) (2016). River Analysis System HEC-RAS user's Manual, Version 5.0, U.S. Army Corps of Engineers Hydrologic Engineering Center, Davis, CA.

Department of Statistics(DOS) (2018) Jordan In Figures. http://dosweb.dos.gov.jo/ar/products/jordan-in-figure2018/. Accessed 9 June 2020.

Department of Statistics (DOS) (2020). http://dosweb.dos.gov.jo/ar/population/population-2/ . Accessed 9 June 2020.

Derdour A. and Bouanani A. (2019). Coupling HEC-RAS and HEC-HMS in rainfall–runoff modeling and evaluating floodplain inundation maps in arid environments: case study of   Ain Sefra city, Ksour Mountain. SW of Algeria. Environmental Earth Sciences. 78(19):586. https://doi.org/10.1007/s12665-019-8604-6.

Derdour, A., Bouanani A., Baba-Hamed, K. (2017). Hydrological modeling in semi-arid region using HEC-HMS model. Case study in Ain Sefra watershed, Ksour Mountains (SW, Algeria). Journal of Fundamental and Applied Sciences 92: 1027–1049. https://doi.org/10.4314/jfas.v9i2.27.

Dupont, B. S. and Allen, D. L. (1999). Revision of the Rainfall Intensity Duration Curves for the Commonwealth of Kentucky. Kentucky Transportation Center Research Report. 292.https://uknowledge.uky.edu/ktc_researchreports/292.

Echogdali, F.Z., Boutaleb, S., Elmouden, A., Ouchchen, M. (2018). Assessing Flood Hazard at River Basin Scale: Comparison between HECRASWMS and Flood Hazard Index (FHI) Methods Applied to El Maleh Basin, Morocco. Journal of Water Resource and Protection 10: 957-977. https://doi.org/10.4236/jwarp.2018.109056.

El Alfy, M. (2016). Assessing the impact of arid area urbanization on flash floods using GIS, remote sensing, and HEC-HMS rainfall–runoff modeling. Hydrology Research 47(6): 1142–1160. https://doi:10.2166/nh.2016.133.

Farhan, Y. and Anabr, A. (2016). Flash Flood Risk Estimation of Wadi Yutum (Southern Jordan) Watershed Using GIS Based Morphometric Analysis and Remote Sensing Techniques: Open Journal of Modern Hydrology 6: 79-100.

Hyarat, T. (2016). Disaster Management, Flood Hazard and Risk Assessment: Case Study Wadi Al Arab Basin, M.S. thesis, The University of Jordan.

Hoseini, Y., Azari, A., Pilpayeh, A. (2017). Flood modeling using WMS model for determining peak flood discharge in southwest Iran case study: Simili basin in Khuzestan Province.

Applied Water Science 7: 3355–3363. https://DOI 10.1007/s13201-016-0482-4.

Hunting Technical Services, Soil Survey and Land Research Centre (HTS and SSLRC) 1993. The Soils of Jordan. Ministry of Agriculture, National Soil Map and Land Use Project, Level 1: Reconnaissance Soil Survey (Scale 1: 250,000), 3 Volumes, Amman.

Ibitoye, M.O., Komolafe, A.A., Adegboyega, A.S., Adebola, A. O., Oladeji, O. D. (2020). Analysis of vulnerable urban properties within river Ala floodplain in Akure, Southwestern Nigeria. Spatial Information Research 28: 431–445. https://doi.org/10.1007/s41324-019-00298-6.

Mancini, C.P., Lollai, S., Volpi, E., Fiori, A. (2020). Flood Modeling and Groundwater Flooding in Urbanized Reclamation Areas: The Case of Rome (Italy). Water 12(7): 2030. https://doi.org/10.3390/w12072030

Marko, K., Elfeki, A., Alamri, N., Chaabani, A. (2019). Two Dimensional Flood Inundation Modelling in Urban Areas Using WMS, HEC-RAS and GIS (Case Study in Jeddah City, Saudi Arabia). Advances in Science, Technology and Innovation 265–267. Published in: Advances in Remote Sensing and Geo Informatics Applications.

Ministry of Water and Irrigation (MWI), (2018). Daily Rainfall Data, Open files.

Moh'd, B. (2000). The geology of Irbid and Ash Shuna Ash Shamaliyya (Waqqas) map sheet no. 3154-II and 3154-III. Natural Resources Authority, Geol. Mapping Division, Bull. 46.

Niyazi, B. A., Masoud, M. H., Ahmed, M., Basahi, J. M., Rashed, M. A. (2020). Runoff assessment and modeling in arid regions by integration of watershed and hydrologic models with GIS techniques. Journal of African Earth Sciences 172. 103966. https://doi:10.1016/j.jafrearsci.2020.103966.

Pregnolato M., Ford A., Wilkinson S., Dawson, R. (2017) The impact of flooding on road transport: A depth-disruption function. Transportation Research Part D 55 (2017): 67–81.

Sadrolashrafi, S.S., Samadi, A., Rodzi, M.A., Thamer, A.M. (2008). Flood Modeling using WMS Software: A Case Study of the Dez River Basin, Iran. In: Altinakar, M.S., Kokpinar, M.A., Darama, Y., Yegen, E.B., Harm A. (Eds.), River Flow. Kubaba Congress Department and Travel Services, Turkey.

SCS U (1986). Urban hydrology for small watersheds, technical release no. 55 (TR-55). US Department of Agriculture, US Government Printing Office, Washington, DC.

UNHCR, (2018). Cash in hand- Urban refugees, the right to work, and UNHCR's advocacy

activities. Available at: https://reliefweb.int/report/egypt/cash-hand-urban-refugees-right-work   and-unhcrs-dvocacy-activities.

World Food Programme (WFP) (2019) Flood Hazard Map Integrated Context Analysis Jordan July 2019.

Youssef, A. and Hegab, M. (2019). Flood-Hazard Assessment Modeling Using Multicriteria Analysis and GIS: A Case Study—Ras Gharib Area, Egypt. Spatial Modeling in GIS and R for Earth and Environmental Sciences 2019: 229-257. https://doi.org/10.1016/B978-0-12-815226-3.00010-7.